Supporting Information

Oxygen vacancy engineered $SrTiO_3$ nanofibers for enhanced photocatalytic H_2 production

Chuan-Qi Li,[a,b] Sha-Sha Yi,*[a,c] De-Liang Chen,[a] Yan Liu,[b] Ya-Jie Li,[b] Si-Yu Lu,[b] Xin-Zheng Yue,*[,b,c] and Zhong-Yi Liu*[,b,c]

[a]School of Materials Science and Engineering, Zhengzhou University, Zhengzhou 450001, China.

[b]College of Chemistry and Molecular Engineering, Zhengzhou University, Zhengzhou 450001, China.

[c]Henan Institutes of Advanced Technology, Zhengzhou University, 97 Wenhua Road, Zhengzhou 450003, China.

*Corresponding author: Sha-Sha Yi

E-mail: yiss@zzu.edu.cn

1. Experimental section

1.1 Synthesis of $SrTiO_3$ nanofibers (NFs): A simple electrospinning method was employed to fabricate the $SrTiO_3$ (STO) NFs. In a typical process, certain amount of polyvinylpyrrolidone (PVP, average molecular weight of 1.3×10^6) and strontium nitrate ($Sr(NO_3)_2$, ≥99.5%) were first dissolved into the mixed solution including 1.5 mL of ethanol (CH_3CH_2OH, ≥95.0%), 1.5 mL of N,N-dimethylformamide (DMF, ≥99.5%), 1.5 mL of acetic acid (≥99.8%), 1 mL of deionized water (18.2 MΩ·cm), and 0.3 mL of tetrabutyl titanate (TBOT, ≥98.0%). After various stirring for 48 h at room temperature, the obtained transparent pale yellow solution was injected into the syringe in a controlled electrospinning setup. The vertical distance between the nozzle tip and the grounded stainless collector and the voltage were conducted at 16 cm and 15 kV, respectively. After several hours later, calcination was performed at 600°C for 3 h at a heating rate of 2°C min^{-1} in air atmosphere to convert the collected white product into STO NFs, labeled as STO-A.

1.2 Thermal treatment on STO-A: STO-A NFs were treated by H_2/N_2 atmosphere (20 vol% in H_2) in the vacuum tube furnace at different heating temperature and reaction time, respectively, varying in the range of 400-1000°C (T) and 1-3 h (t). The as-prepared specimens were named as STO-NH. For comparison, STO-A photocatalyst treated in N_2 atmosphere (99.999%) at 600°C for 3 h was also prepared, labeled as STO-N.

1.3 Characterization: The field emission scanning electron microscope (FESEM) images were obtained with a JEOL JSM 6700F electron microscope. The transmission electron microscopy (TEM) and high-resolution TEM (HRTEM) images were conducted on a Tecnai G2 S-Twin F20 TEM microscope (FEI Company). The energy-dispersive X-ray (EDX) spectroscopy, the scanning TEM-EDX element mapping, and the selected area electron diffraction (SAED) were carried out on a HITACHI SU-8020 transmission electron microscopy. The crystalline

structure of the as-prepared samples was characterized by powder X-ray diffraction (XRD) with a Rigaku D/Max-2550 diffractometer using Cu Kα radiation (λ = 1.54056 Å) at 50 kV and 200 mA in the 2θ range of 20-80° at a scanning rate of 4 and 0.5° min^{-1}, respectively. X-ray photoelectron spectroscopy (XPS) measurements were performed on a Thermo VG Scientific ESCALAB 250 spectrometer using monochromatized Al Kα excitation. The UV-visible diffuse reflectance spectra (UV-vis DRS) of the samples were measured on a UV-vis-NIR spectrophotometer (Shimadzu UV-3600) detecting absorption over the range of 300-800 nm. The steady-state photoluminescence (PL) emission spectra with an excitation wavelength of 350 nm were measured on a FLUOROMAX-4. The electron paramagnetic resonance (EPR) spectra were collected using a BRUCER EMXplus-9.5/12 spectrometer at 9.44 GHz at 300 K.

1.4 Photocatalytic H_2 production from water reduction: The photocatalytic H_2 production experiments were performed at atmospheric pressure in a 300 mL Pyrex glass reaction cell containing 25 mg of photocatalyst, 90 mL of H_2O and 10 mL of triethanolamine (TEOA, 98%), in which TEOA was used as a sacrificial reagent. Before reaction, the mixture solution was sonicated for 10 min in an ultrasonic bath to get uniform suspension. Then, a 300 W Xe lamp with cooling water (stabilize the temperature at 277 K) was served as the simulated solar light source to trigger the photocatalytic reaction and the suspension was continuously stirred to ensure uniform irradiation. H_2 gas production was analyzed using an online gas chromatograph (GC-8A, Shimadzu Co., Japan, with N_2 as the carrier gas) equipped with an MS-5A column and a thermal conductivity detector (TCD). The stability test was performed by using the method mentioned above under the same condition. Once the photocatalytic reaction of a cycle test of 4 h was completed, the second cycle was performed after the reactor was fully degassed in vacuum. Before the third cycle begins, 10 mL of TEOA was added into the reaction. Finally, the test was performed for 4 cycles.

The apparent quantum efficiency (AQE) was measured on STO-NH specimen under

monochromatic light irradiation of 365 nm according to the following equation S1:[14]

$$AQE(\%) = \frac{2 \times Number\ of\ evolved\ H_2\ molecules}{Number\ of\ incident\ photons} \times 100 = \frac{2 \times N_1}{N_2} \times 100 \qquad (S1)$$

where N_1 and N_2 represent the number of evolved H_2 molecules and number of incident photons, respectively.

1.5. Electrochemical and photoelectrochemical measurements: Typically, the electrochemical and photoelectrochemical (PEC) measurements were performed in a three-electrode system by employing an electrochemical analyzer (CHI760E Instruments), in which the as-prepared specimen film, Pt wire and Ag/AgCl (saturated KCl) were served as the working electrode, counter electrode and reference electrode, respectively. In this work, the working electrodes includes STO-A, STO-N and STO-NH sepcimen films, seen the preparation method as described in earlier report.[S1] All the electrochemical and PEC measurements were carried out in potassium hydroxide (KOH, ≥90%) aqueous solution (1 M, pH = 13.6). For PEC reaction, the simulated solar light was generated with a 300 W Xe lamp (CEL-HXF300, Beijing China Education Au-light Co., Ltd) equipped with an AM 1.5G optical filter. Electrochemical impedance spectroscopy (EIS) were performed under light irradiation with 5 mV perturbation and a frequency range from 100 kHz to 0.1 Hz at potential of 0 V *vs*. Ag/AgCl. Mott-Schottky (M-S) plots were performed and recorded over an AC frequency of 1 kHz in dark condition to judge the characteristic of semiconductor types as well as obtain their flat band potentials. Open circuit potential (OCP) decay curves were collected after turning off the light irradiation, analyzing the charge decay behaviors in the photocatalysts. Current-time (*i*-*t*) curves were performed on a light turn-on/off system with an applied potential of 0 V *vs*. Ag/AgCl.

2. Supplemental Figures and Tables

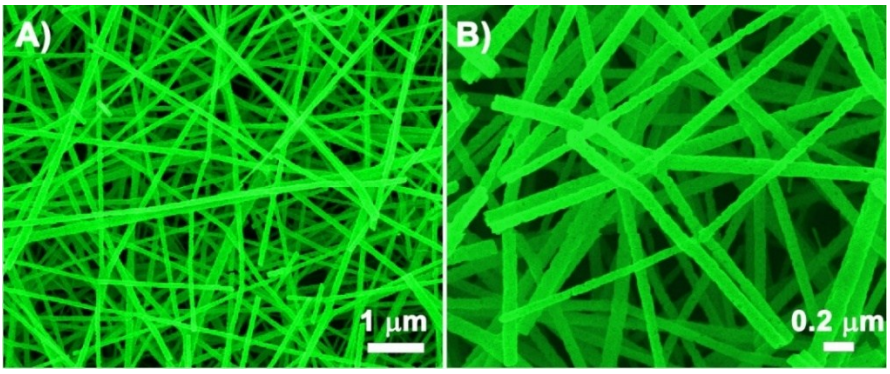

Fig. S1 FESEM images of STO-A in (A) low- and (B) high-magnification.

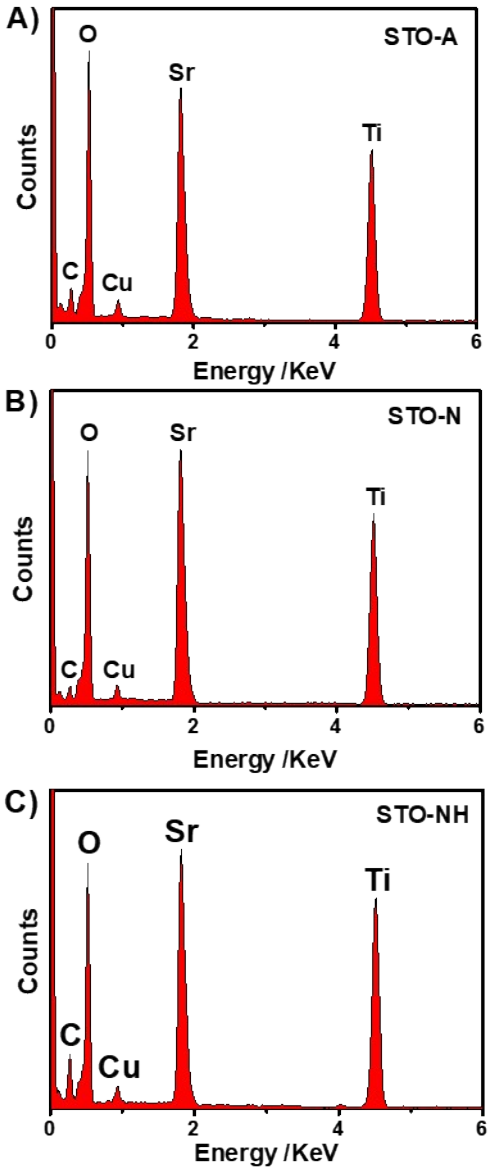

Fig. S2 EDX spectra of (A) STO-A, (B) STO-N and (C) STO-NH.

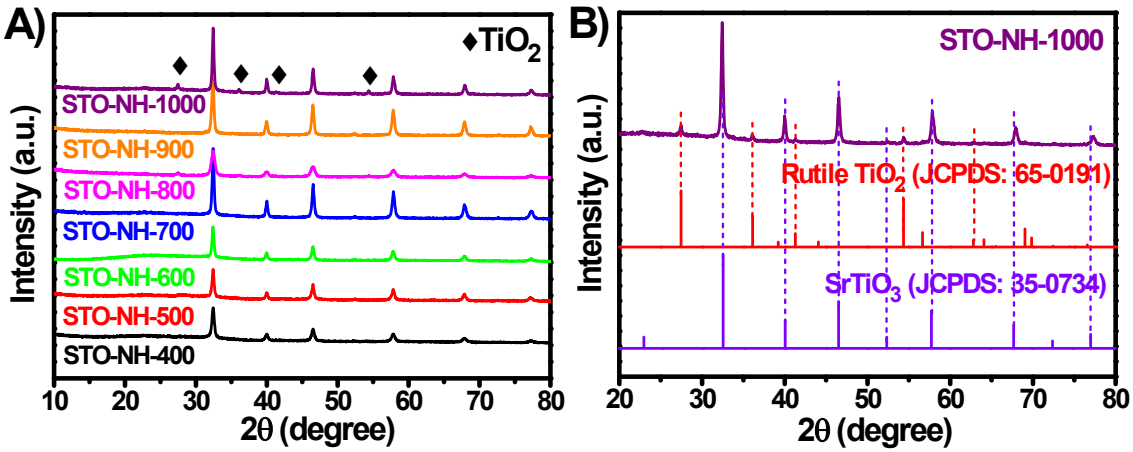

Fig. S3 XRD patterns of (A) STO-NH prepared at different reaction temperature from 400 to 1000°C and (B) STO-NH obtained at 1000°C.

Fig. S3 demonstrates the STO-NH specimens prepared at different reaction temperature from 400 to 1000°C. It can be seen that no impurity phases are observed for STO-NH-T (where T is 400, 500, 600, 700, 800 and 900°C), and all the peaks can be well-indexed to the $SrTiO_3$ (JCPDS No. 35-0734). While a set of additional diffraction peaks can be observed on STO-NH sample obtained at 1000°C as compared to other STO-NH specimens (Fig. S3B), of which can be assigned to the rutile phase of TiO_2 (JCPDS No. 65-0191).

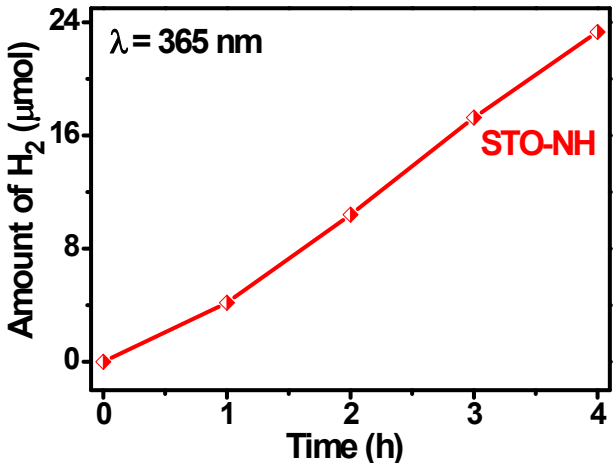

Fig. S4 Typical time course of H_2 production of STO-NH at 365 nm in 10 vol% TEOA aqueous solution.

To achieve the apparent quantum efficiency (AQE) of STO-NH, the photocatalytic H_2 production test was performed under monochromatic light irradiation of 365 nm in 10 vol% TEOA aqueous solution, as shown in Fig. S4. The average incident light intensity and irradiation area are measured to be 5.34 mW cm^{-2} and 28.27 cm^2, respectively.

In addition, the amount of H_2 production of STO-NH was collected to be 23.32 μmol during the irradiation of 4 h. Thus, the number of evolved H_2 molecules (N_1) was calculated to be $9.74 \times 10^{14}\ molecule\ s^{-1}$ according to $N_1 = N_A \times M$, wherein N_A is the Avogadro's constant (6.02×10^{23} molecules mol^{-1}) and M is the average H_2 generation rate (mol s^{-1}).

To obtain the number of incident photons (N_2), the equation of $N_2 = \frac{E\lambda}{hc}$ is adopted. As a result, the calculated value of N_2 is 2.77×10^{17} photons s^{-1}, wherein E is the power of lamp source, h is the Planck's constant (6.63×10^{-34} J·s), and c is the speed of light (3.0×10^8 m s^{-1}).

As a result, the AQE of STO-NH was calculated to be 0.70% according equation S1.

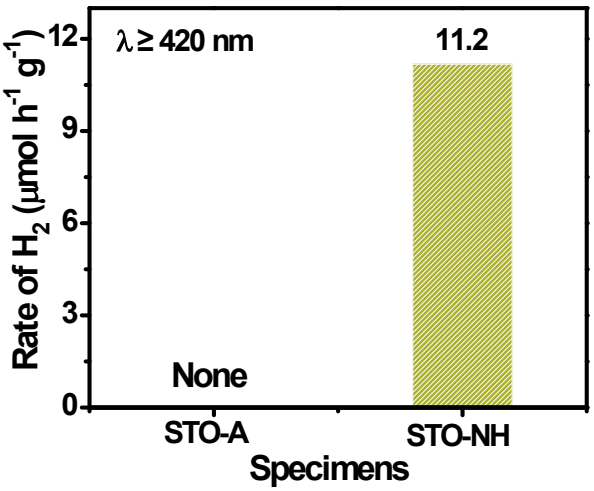

Fig. S5 Photocatalytic H_2 production rates of STO-A and STO-NH specimens under visible light irradiation ($\lambda \geq 420$ nm).

To verify how the enhanced light harvesting ability influence the photocatalytic performance of STO-NH, Fig. S5 compares the photocatalytic H_2 production rates of STO-A and ATO-NH under visible light irradiation ($\lambda \geq 420$ nm). As a result, no H_2 was detected on STO-A, while STO-NH showed the low H_2 production rate of 11.2 μmol h^{-1} g^{-1}.

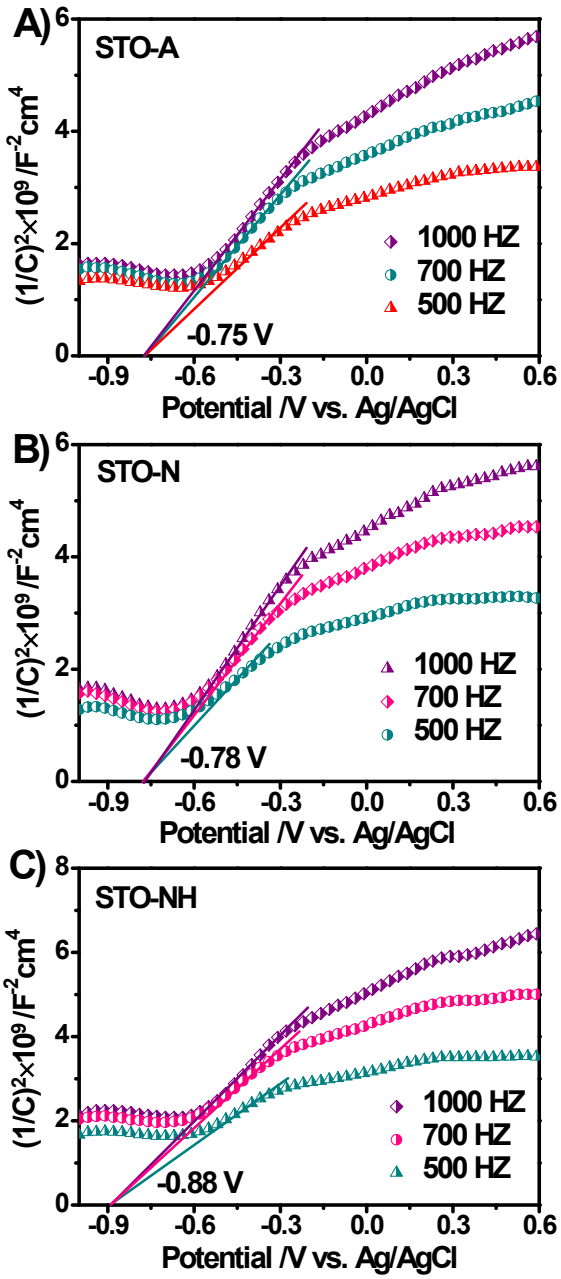

Fig. S6 M-S plots of (A) STO-A, (B) STO-N, and (C) STO-NH specimens under various frequencies of 500, 700 and 1000 Hz in dark condition.

As shown in Fig. S6, the Mott-Schottky (M-S) plots of STO-A, STO-N, and STO-NH electrodes are conducted and recorded over an AC frequencies of 500, 700 and 1000 Hz in dark. The flat band potentials (E_{fb}) of these materials are estimated according to the following equation S2:[S2]

$$\frac{1}{C^2} = \frac{2}{e\varepsilon\varepsilon_0 N_D}\left[\left(E - E_{fb}\right) - \frac{\kappa T}{e}\right] \qquad (S2)$$

where C is the space charge capacitance, ε_0 is the relative dielectric constant of $SrTiO_3$, ε is the vacuum permittivity (8.85×10^{-12} F m^{-1}), N_D is the charge donor density (cm^{-3}), E is the electrode applied potential, E_{fb} is the flat band potential, κ is the Boltzmann's constant (1.38×10^{-23} J K^{-1}), T is the absolute temperature (in K) which is generally small and could be neglected, and e is the electron charge.

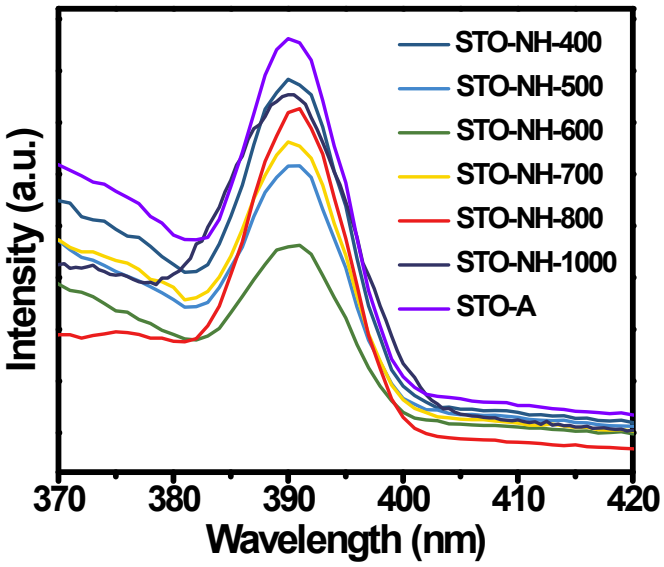

Fig. S7 PL spectra of STO-NH prepared at different temperature range from 400 to 1000°C.

Fig. S7 shows the PL emission peaks for STO-NH samples obtained by treating STO-A in H_2/N_2 atmosphere under the temperature range from 400 to 1000°C. It can be seen that, as compared to STO-A, the PL peak intensity significantly decreased with the increase of treatment temperature and reaches a minimum at 600°C. The above result suggests that the highest separation of charge carriers is achieved when the treatment temperature is 600°C. That is to say, increasing the treatment temperature above 600°C can not bring about further separation of electron-hole pairs. These results are agreement with the photocatalytic performances (Fig. 4A).

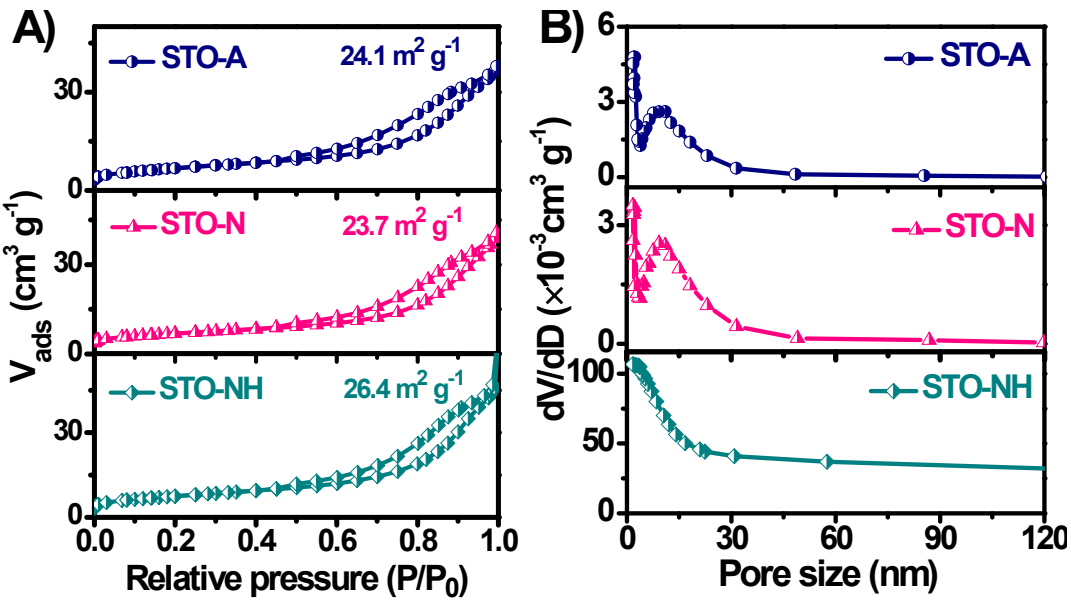

Fig. S8 (A) N_2 adsorption-desorption isotherms and (B) BJH pore size distribution of STO-A, STO-N and STO-NH specimens.

To study how the thermal treatment affects the Brunauer-Emmett-Teller (BET) surface areas and porous structures, the N_2 adsorption-desorption isotherms and BJH pore size distributions for STO-A, STO-N and STO-NH photocatalysts are carried out. As illustrated in Fig. S8, the isotherms of all the samples belong to type IV physisorption isotherm and exhibit H3-type hysteresis behavior,[S3] indicating the presence of mesopores. The specific surface areas of STO-A, STO-N and STO-NH are 24.1, 23.7 and 26.4 m^2 g^{-1}, respectively, meaning that the introduction of OVs can not improve the surface area of STO-A.

Table S1 Comparison of the catalytic activities and preparation methods for the defective $SrTiO_3$-based photocatalysts reported recently.

Catalyst	Photocatalytic performance	Photocatalytic reaction condition	Cocatalyst	Preparation method	Ref.
Oxygen vacancy $SrTiO_{3-x}$	2286 μmol h^{-1} g^{-1}	400 W high-pressure Hg lamp; pH 12; Glucose = 1.0 g L^{-1}	0.5 wt% Pt	Treatment at 400ºC in 5% H_2/N_2 mixed gas flow	24
$SrTiO_3$ nanocubes	6236 μmol h^{-1} g^{-1}	300 W Xe lamp	1 wt% Pt	$SrCO_3$, Ti powder, TiO_2, NaCl and KCl were annealed at 700ºC in air	S4
$SrTiO_3$@$SrTiO_{3-x}$	2200 μmol h^{-1} g^{-1}	300 W Xe lamp, aqueous methanol solution (25 vol %)	1 wt% Pt	Reaction with $NaBH_4$ at 325ºC in Ar	35
Ti^{3+} defects in $SrTiO_3$	2250 μmol h^{-1} g^{-1}	300 W Xe lamp, aqueous methanol solution (25 vol%)	9.6% to 14.7% (Pt:Ti)	Annealed at 1000ºC in tube furnace	S5
H:$SrTiO_3$	708 μmol h^{-1} g^{-1}	300 W Xe lamp, aqueous CH_3OH solution (20 vol%),.	0.5 wt% Pt	Reaction with $NaBH_4$ at 350ºC in N_2	S6
Self-doped $SrTiO_{3-\delta}$ powders	-	300 W Xe lamp	0.3 wt% Pt	Anneal in Ar from 1200 to 1400ºC	S7
La and Cr co-doped $SrTiO_3$	20 μmol h^{-1} g^{-1}	Visible light irradiation (≥ 420 nm), 5 M NaOH solution filled with methanol (10 vol%)	1.0 wt% Pt or PtO_x	Calcined at 1000 ºC for 12 h and fired at 1250ºC for 16 h	S8
$SrTiO_3$ single crystals (HSTONP-700)	0.15 μmol g^{-1} h^{-1}	300 W Xe lamp, aqueous methanol solution (50 vol %)	None	Treatment at 700ºC in H_2 gas (Linde, 99.99%)	29
Oxygen vacancy engineered $SrTiO_3$ nanofibers	330 μmol h^{-1} g^{-1}	300 W Xe lamp, triethanolamine solution (10 vol%)	None	Hydrogen treatment at 600ºC in 20% H_2/N_2 mixed gas flow	This work

3. Supplemental references

[S1] X. Yue, S. Yi, R. Wang, Z. Zhang and S. Qiu, *J. Mater. Chem. A* 2017, ***5***, 10591-10598.

[S2] X. J. Wen, C. G. Niu, L. Zhang, C. Liang and G. M. Zeng, *J. Catal.* 2017, ***356***, 283-299.

[S3] K. S. W. Sing, *Pure Appl. Chem.* 1982, ***54***, 2201-2218.

[S4] G. Zhang, W. Jiang, S. Hua, H. Zhao, L. Zhang and Z. Sun, *Nanoscale.* 2016, **8**, 16963-16968.

[S5] H. Chen, F. Zhang, W. Zhang, Y. Du and G. Li, *Appl. Phys. Lett.* 2018, **112**, 013901.

[S6] B. Wang, S. Shen and L. Guo, *ChemCatChem.* 2016, **8**, 798-804.

[S7] K. Xie, N. Umezawa, N. Zhang, P. Reunchan, Y. Zhang and J. Ye, *Energy Environ. Sci.* 2011, **4**, 4211-4219.

[S8] J. Hui, G. Zhang, C. Ni and J. T. S. Irvine, *Chem. Commun.* 2017, **53**, 10038-10041.